34th Annual International Conference of the IEEE EMBS
San Diego, California USA, 28 August - 1 September, 2012

Quantification of Cy-5 siRNA Signal in the Intra-vital Multi-photon Microscopy Images

Antong Chen, Belma Dogdas, Saurin Mehta, Kathleen Haskell, Bruce Ng, Ed Keough, Bonnie Howell, D. Adam Meacham, Amy G. Aslamkhan, Joseph Davide, Matthew Stanton, Ansuman Bagchi, Laura Sepp-Lorenzino, and Weikang Tao

Abstract—**Transgenic mice with Tie2- green fluorescent protein (GFP) are used as a model to study the kinetic distribution of the Cy5-siRNA delivered by lipid nanoparticles (LNP) into the liver. After the mouse is injected with the LNP, it undergoes a procedure of intra-vital multi-photon microscopy imaging over a period of two hours, during which the process for the nanoparticle to diffuse into the hepatocytes from the vasculature system is monitored. Since the images are obtained in-vivo, the quantification of Cy5 kinetics suffers from the moving field of view (FOV). A method is proposed to register the sequence of images through template matching. Based on the semi-automatic segmentations of the vessels in the common FOV, the registered images are segmented into three regions of interest (ROI) in which the Cy5 signals are quantified. Computation of the percentage signal strength in the ROIs over time allows for the analysis of the diffusion of Cy5-siRNA into the hepatocytes, and helps demonstrate the effectiveness of the Cy5-siRNA delivery vehicle.**

I. INTRODUCTION

Transgenic mice with Tie2-GFP provide a promising model to study the delivery of Cy5-siRNA to the hepatocytes via the liver vasculature system [1]. With the LNP as the delivery vehicle, the Cy5-siRNA is transferred into the vessels, and diffused into the surrounding hepatocytes in a period of up to 2 hours. The process is monitored using an intra-vital multi-photon microscopy system [2, 3]. Due to the high resolution (up to 0.2 μm) of the imaging technique, structure of the vasculature system and the hepatocytes can be observed at the cellular level.

Since in multi-photon microscopy the florescence excitation only occurs where two photons are absorbed simultaneously, each of the photons can be delivered individually with less energy. Consequently, the scattering on each of their paths is drastically reduced, leading to an improved penetration of up to 1mm, compared with the penetration of around tens of microns in traditional confocal microscopy. Therefore, the multi-photon microscopy allows images to be taken at spots inside the liver of the mouse *in-vivo*, and facilitates monitoring of the Cy5-SiRNA diffusion in real time. Using video-microscopy, colored images are obtained at time points in a span of two hours, forming an image sequence. In each of the images, as it is shown in Figure 1, the blue channel displays the nuclei of the hepatocytes, the green channel shows the vascular endothelial cells, and the red channel illustrates the Cy5 signal which is either inside the vessel, concentrated on the endothelial layer, or diffused into the hepatocytes. Quantifying the Cy5 signal strength in the three ROIs over time can describe the kinetics of the siRNA delivery. However, due to the movement of the animal in the imaging process, the accuracy of the quantification is undermined. As the FOV is not consistent between frames, registration of the frames in the image sequence becomes necessary, such that a common FOV can be found, and the Cy5-siRNA signal strength within this common region over time can be quantified. Similar to the strategy proposed in [4], the registration implemented herein is based on intensity-based template matching, which involves registering the frames in the image sequence to a common target image. A common FOV is then established in the registered images for all subsequent analyses.

To quantify the signal strength inside the FOV, images are first segmented into three ROIs, including the inside of the vessels, the vessel wall, and the hepatocytes. Percentage of signal inside each ROI is calculated over time.

II. METHODS AND MATERIALS

A. Imaging Procedure

Tie2-GFP transgenic mice were purchased from the Jackson Laboratories. Mice were anesthetized with ketamine/xylazine (Ketamine/xylazine at 50-200/3-10 mg/kg, IM/IP) then intubated with 30 G catheter over a guide wire under direct visualization and ventilated at a rate of 100 breaths/min with a tidal volume of 0.25 ml. The tail vein was

A. Chen, *B. Dogdas, S. Mehta, A. Bagchi are with the Informatics IT, Merck Research Labs IT, Rahway, NJ 07065, USA (e-mail: belma_dogdas@merck.com).

K. Haskell, B. Ng, E. Keough, J. Davide, L. Sepp-Lorenzino, and W. Tao are with the Department of RNA Therapeutics, Merck Research Labs, West Point, PA 19486, USA.

B. Howell is with the Molecular Biomarkers, Merck Research Labs, West Point, PA 19486, USA.

D. A. Meacham and A. G. Aslamkhan are with the [4]Molecular and Investigational Toxicology, Merck Research Labs, West Point, PA 19486, USA.

M. Stanton is with the Medicinal Chemistry, Merck Research Labs, West Point, PA 19486, USA.

cannulated for venous access with a 30 G needle attached to P10 tubing. An incision was placed in the abdominal cavity just below the ribcage and the liver was exteriorized. A Fluorodish (World Precision Instruments, Sarasota, FL) was placed over the incision and the animal was turned over to let the organ to fall in to the Fluorodish. The animal was set atop the stage of the LSM 510 NLO META-confocal microscope (Zeiss, Jena, Germany) equipped with a Chameleon multiphoton laser (Coherent, Santa Clara, CA). A circulating warm water heating pad was placed over the stage of the microscope. Temporary cessation of breathing was achieved by maintaining expiratory pressure with the use of pressure transducer in the ventilation system, which would allow stable image to be taken at 40x objective magnification. 100 µl of 0.5 mg/ml Hoechst 3342 (Invitrogen, Carlsbad, CA) was administered via the tail vein cannula to stain nucleus. Images were collected using the 488 (excites GFP), 663 (excites Cy5) and 780 nm (2 photon, excites Hoechst) excitation wavelengths and emission wavelength windows of 500-550 nm (bandpass, collect for GFP), 651-694 nm (META channel, collect for Cy5), and 435-485 nm (bandpass, collect for Hoechst) respectively.

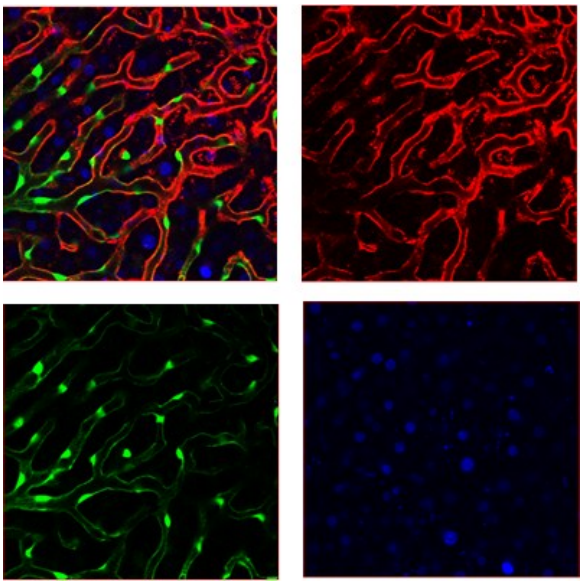

Figure 1. Example of an intra-vital microscopy image obtained in the experiment. The original image is shown at the top left, the top right the red channel, the bottom left the green channel, and the bottom right the blue channel.

A pre-dose image is first obtained before the Cy5 dose is applied, in which only the green channel and the blue channel are observable for the vasculature and the nuclei of the hepatocytes, respectively. Meanwhile, the time is set to 0. After the injection of the LNP solution, an image is first taken at the point of 5min, when the Cy5 signal (observable in the red channel) start to appear mainly inside the vessels.

With the objective fixed, an image is taken every 5 min in the first 15 minutes. Beyond 15min, images are obtained every 15min until 120min. Thus the entire sequence consists of 11 images obtained at 11 time points in a period of 2 hours. The size of the FOV on the subjects is about 2.16mm×2.16mm, and the depth is 50 – 100 microns. The left column of Figure 2 shows images in the sequence for one subject, which were obtained at 0, 15, 60, and 120 min. Colored images are saved as 512×512 TIFF files with pixel size of 0.169mm×0.169mm.

B. Image Registration

Since the mouse was alive in the two-hour imaging procedure, the recorded image sequence suffered from a moving FOV caused by respiratory and body movements. As it is shown in the left column in Figure 2, a circle is drawn at a location in the image obtained at 60min. With the circle copied onto the other three images, the structure encompassed at the same position varies. Similar to the registration of microscopy images, as reported in [4], the movement observed in our data is mainly translational shifting. Therefore we apply a translational template matching based on the intensity of the source and target images. First, an image in the sequence is assigned as the target image onto which all other source images are registered. Since the shifting observed is mostly in one direction, we opt to select the image at the middle of the sequence, i.e. image obtained at the 60min, as the target such that the registered images tend to share a common FOV with maximum size.

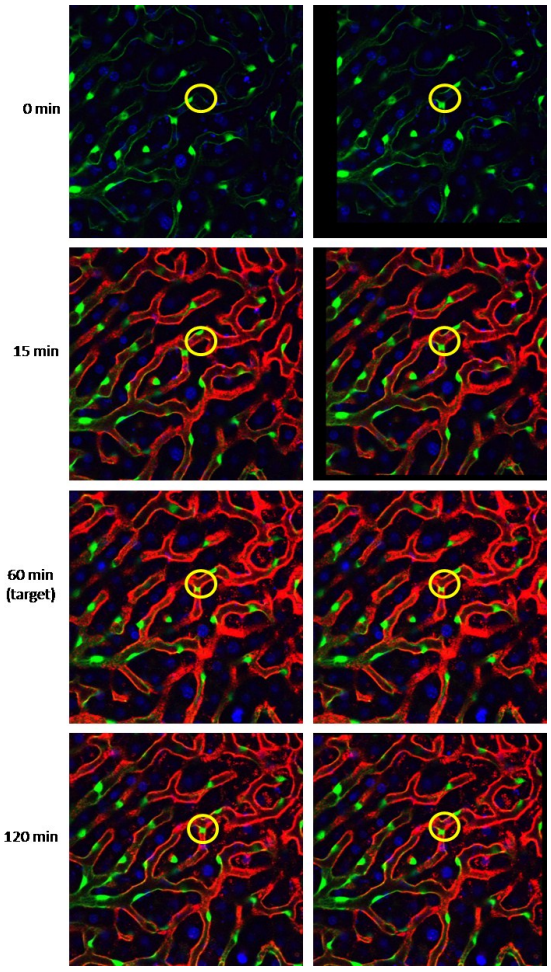

Figure 2. Original unregistered (left column) and registered images (right column). As the image at 60min was selected as the target, a yellow circle is drawn on it and copied onto the same location of other images. Similar contents are seen in the circles for the registered images, while the contents observed are different in the circles for unregistered images.

A template is then selected on the target image as a rectangular region fulfilling the following requirements: (1) Must contain characteristic structural information, e.g. vessel branching and conjunction. (2) Must have a proper size and location, such that its corresponding regions are observable in all frames of the image sequence. Since in the colored images, the blue channel contains only the nuclei, whose patterns are indistinctive, and the red channel mutates over time due to the diffusion of the probes, the green channel provides the ideal characteristics for the template.

Once manually assigned on the target image, the corresponding regions in the rest of the images are found by searching in a user-defined rectangular region. An exhaustive search is implemented herein since the search space is not enormous. Using cross correlation (CC) as a measure of similarity, the region with the highest similarity is matched to the template, and the coordinate difference between the region and the template is used to calculate the shift *T*. Figure 2 shows the registered images as a comparison to the original images. Evidently, same structures are seen in the circles drawn on the target image, indicating that images are aligned correctly.

C. *Automatic Template Matching*

To reduce the manual interaction in the selection of template and search region, we propose an automatic template selection method as an alternative. First, as it is shown in Figure 3, the entropy of the image is calculated, generating an entropy map. Second, since it is more optimal to place the template closer to the center of the target image, such that its corresponding regions in the other images are less likely to be out of the FOV, a position map, essentially a Gaussian kernel placed at the center of the image, is applied to the entropy map. Finally, the region with the highest weighted entropy is selected as the template. Since regions only containing vessels or hepatocytes tend to have lower entropy, the proposed method can automatically detect regions with a balance between both types of tissues, and meets the requirements for templates described in section II.B.

D. Vessel Segmentation

The segmentation of the vessels from the hepatocytes is initiated by Otsu's optimal thresholding method [5] on the green channel images. Later, vessel segmentations are filled using morphological operations and corrected manually. The processing was performed using Definiens software suite (Definiens AG, Munich, Germany). Results are saved as binary masks.

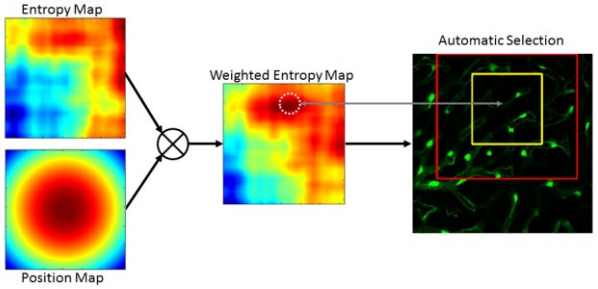

Figure 3. Procedure for automatic template selection.

E. *Determination of ROIs*

In the typical Cy5 diffusion, when a steady state is reached in the endothelial layer, the Cy5 concentration will remain stable near the vessel wall, while the concentration inside the vessels will decrease as the LNP diffuses into the hepatocytes. Therefore to accurately study the kinetics of the Cy5 delivery, we segmented the image into three ROIs: The hepatocytes, the vessel wall, and the inside of the vessel. Based on the binary segmentation of the vessels, we first use morphometric erosion to shrink the mask of vessels, such that it only contains the inside region of the vessels. We then dilate the mask, and subtract the eroded mask to obtain a mask for the region of the vessel walls. Excluding these two ROIs, the rest of the image belongs to the hepatocytes.

Image binary morphometry is implemented to the vessel mask with a square structuring element of 3×3 pixels, such that each erosion/dilation can remove/expand the current mask for only 1 pixel. However, the exact number of iterations in the erosion/dilation will affect the segmentation accuracy of the ROIs directly.

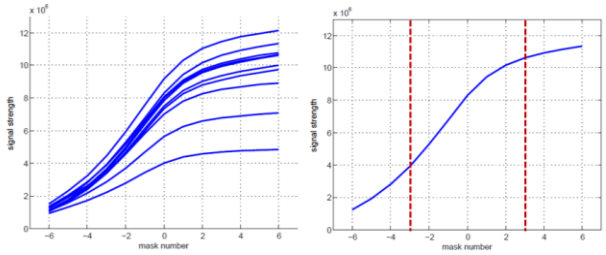

(a) (b)

Figure 4. Impact of dilating and eroding the mask on the measurement of Cy5 signal strength inside the masks. Negative numbers on the *x*-axis represent the eroded masks, and positive numbers represent the dilated masks. Signal strength for masks at all the time points are shown by the *y*-axis in (a), and the results for the target image (60min) is shown in (b).

We erode the mask for 6 iterations, and also dilate the mask for 6 iterations, recording the Cy5 signal strength in each of the 12 masks, as well as the original mask. The signal strength *S* is calculated as

$$S = \sum_{i,j} I(i,j) \cdot L(i,j) \cdot C(i,j) \qquad (1)$$

where $I(i, j)$ is the intensity in the red channel at pixel (i,j), $L(i, j)$ is the binary label (0 for background and 1 for foreground) determined by the segmentation mask, and $C(i, j)$ is the binary label representing the common area of all registered images. Figure 4(a) shows the effect of eroding or dilating the mask to the signal strength. Since most of the curves show similar trends, indicating similar characteristics for images taken at different time points, we select a representative image at 60min and show its curve in Figure 4(b). It can be seen that the signal strength does not increase much after dilating the original mask for more than 3 pixels. This is because dilating the mask for more than 3 pixels will expand the mask into the hepatocytes region with lower Cy5 concentration. On the other hand, eroding the original mask for more than 3 pixels is continuously reducing the signal strength, while the decreasing rate is becoming lower. This is mainly because that the mask is eroded into the inside of the vessel, in which the Cy5 concentration is relatively lower

than that in the vessel wall region. Therefore, dilating and eroding the original mask for 3 pixels should be able to define the vessel wall region as their difference. Figure 5 shows the images with the dilated and eroded masks applied, as well as the image with the vessel wall as the subtracted difference between the two. Visual inspection of the images implies that the dilation and erosion of 3 pixels are proper.

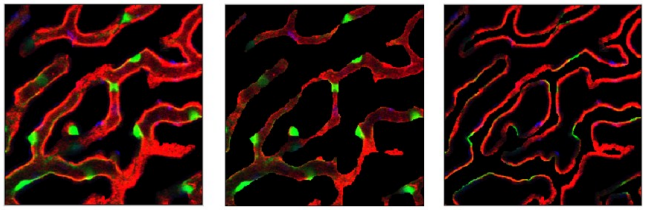

Figure 5. An image after applying the mask dilated for 3 pixels (left panel), image after applying the mask eroded for 3 pixels (middle panel) showing the inside of the vessels, and the image showing the vessel wall (right panel) as a difference between the other two images.

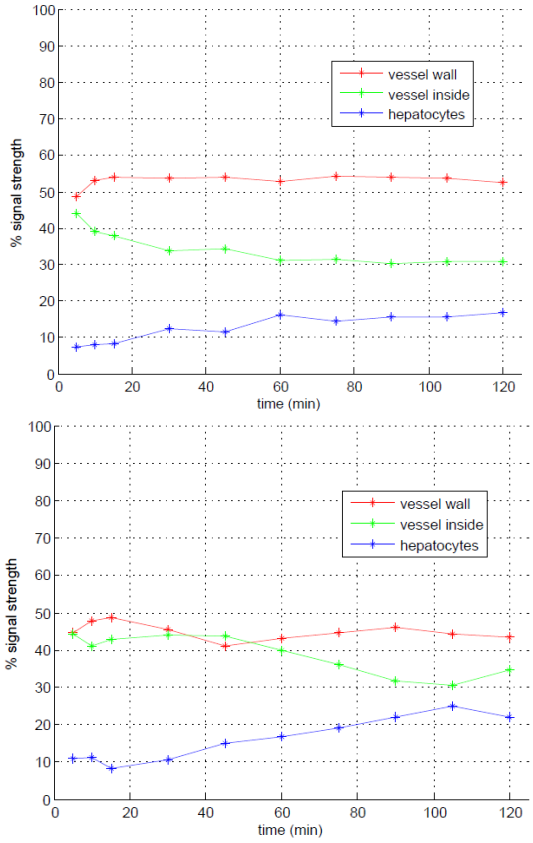

Figure 6. Quantification of Cy5 signal in three ROI's for two subjects.

III. RESULTS

After the ROIs are defined, the Cy5 signal strength in each of the ROIs and the entire image is computed using Equation (1), and the percentage of signal in each ROI in the total is calculated. Results of percentage of signal in each ROI for 11 time points are recorded and plotted in Figure 6 for two subjects. From the plots, we see that the signal inside the vessels is decreasing, and the percentage of signal in the hepatocytes is increasing, while the percentage of signal in the vessel walls remains constant, in general. The trend provides strong evidence that the diffusion of Cy5 was going in a right direction, demonstrating that the delivery vehicle for the Cy5 siRNA was effective.

IV. CONCLUSION AND DISCUSSION

Intra-vital multi-photon microscopy provides a good platform for analyzing the kinetics of the Cy5-siRNA delivery vehicle in the liver of transgenic GFP mice. To analyze the microscopy images, we provided a complete framework for the registration and segmentation of the images. We performed an automatic analysis in a common FOV after correcting the motion of the animal, and identified the ROIs for the inside of the vessels and the vessel walls, and quantified the signal strength inside each of these ROIs as well as the hepatocytes. The percentage of signal strength in each ROI provided an evidence of the effectiveness of the Cy5-siRNA delivery vehicle.

At the current stage, the segmentation of the vessels is semi-automatic. We will work on fully automating the process. Based on the segmentation results from Otsu's thresholding, we could utilize the structural information of the vessel walls specifically from the green channels, and automatically fill the voids inside the vessels.

Further validation of the proposed framework is being performed on more data. Although based on our current dataset, translation is the only transformation considered in the registration, adding more degrees of freedom, e.g. rotation, scaling, and shearing could improve the robustness of the approach on solving possibly more complicated problems in larger dataset. Moreover, the comprehensiveness of the proposed method will also be examined on microscopy of other organs, e.g. the kidney.

REFERENCES

[1] F. Hillen, E. Kaijzel, K. Castermans, *et al*., "A transgenic Tie2-GFP athymic mouse mode: a tool for vascular biology in exnograft tumors," *Biochem. Biophys. Res. Commun.* no. 368, pp. 364-367. 2008.

[2] K. Dunn, R. Sandoval, K. Kelly, *et al*., "Functional studies of the kidney of living animals using multicolor two-photon microscopy," *Am. J. Physiol. Cell Physiol.* no. 283, pp. 905-916. 2002.

[3] K. Dunn and P. Young, "Principles of multiphoton microscopy," *Nephron. Exp. Nephrol*. no. 103, e33–e40. 2006.

[4] J. Lee, A. Jirapatnakul, A. Reeves, *et al*., "Vessel Diameter Measurement from Intravital Microscopy," *Ann Biomed Eng*. no. 37(5), pp. 913–926. 2009.

[5] N. Otsu, "A threshold selection method for gray-level histograms," *IEEE Trans. Sys. Man Cyber*. vol. 9, no. 1, pp. 62-66. 1979.